IEEE Access
Multidisciplinary : Rapid Review : Open Access Journal

Received October 9, 2018, accepted October 29, 2018, date of publication November 9, 2018, date of current version December 19, 2018.

Digital Object Identifier 10.1109/ACCESS.2018.2879157

Study on Degradation of SF_6 in the Presence of H_2O and O_2 Using Dielectric Barrier Discharge

XIAOXING ZHANG[1], ZHAOLUN CUI[1], YALONG LI[1], HANYAN XIAO[2], YI LI[1], AND JU TANG[1]

[1]School of Electrical Engineering, Wuhan University, Wuhan 430072, China
[2]Electric Power Research Institute, State Grid Jiangsu Electric Power Co., Ltd., Nanjing 210008, China

Corresponding author: Xiaoxing Zhang (xiaoxing.zhang@outlook.com)

This was supported by the National Natural Science Foundation of China (NSFC), under Grant 51777144.

ABSTRACT In this paper, a method using dielectric barrier discharge for SF_6 abatement is investigated. The destruction and removal efficiencies (DRE) of plasma abatement of 2% SF_6 in the presence of H_2O and O_2 were studied. The addition of H_2O and O_2 effectively promoted the decomposition process of the SF_6. With the participation of 0.5% H_2O and 2% O_2, the DRE reached 98.2% at 50mL/min flow rate and the energy efficiency reached 5.73 g/kWh. By emission spectra and products composition analysis, we found that the addition of H_2O can generate a large amount of H and OH radicals in plasma region, making SF_6 tend to degrade to produce SO_2. The addition of O_2 can generate a large amount of O radicals, which promotes the production of SO_2F_2. The addition gas not only affects the type of products, but also determines the selectivity of each degradation product. The results in this paper provide experimental support for the treatment of SF_6 tail gas using low temperature plasma.

INDEX TERMS SF_6, DBD, H_2O, O_2, emission spectra, products analysis.

I. INTRODUCTION

As a colorless, odourless and non-toxic gas, SF_6 is widely used in the power industry as the insulating gas because of its excellent insulation properties. However, SF_6 has a very strong greenhouse effect with a globel warming potential up to 23,500 and a stable atmospheric presence of 3,200 years [1]. It was one of the six greenhouse gases listed in the 1997 Kyoto Protocol [2]. In recent years, with the development of the power industry, the demand for SF_6 has been increasing. The electrical field accounts for about 80% of the total demand of SF_6 [3]. In the past five years, the content of SF_6 in the global atmosphere has increased to the order of $\sim 10^5$ tons [4]. Therefore, the emission and treatment of SF_6 is a hot issue in environment field in recent years.

Methods like thermal degradation [5]–[8], photodegradation [9]–[11], catalyst decomposition [12] and electrical degradation have been applied for abating SF_6. The first three methods have disadvantages such as low processing efficiency and harsh reaction conditions, and are not suitable for large-scale industrial use. Electrical degradation methods are based on nonthermal plasmas include microwave discharge, radio frequency discharge, dielectric barrier discharge (DBD) and other means. The active particles in plasma collide with the SF_6 molecule and decompose S-F bonds [13]–[16]. DBD discharge, as a low-temperature plasma, has relatively simple discharge conditions and experimental setup, and is relatively safe to operate. It is widely used to treat VOCs and other industrial tail gases [17]–[19]. In recent years, some scholars have studied the degradation of SF_6 with DBD and the effects of factors such as addtion gases and humidity on the degradation of SF_6 were researched [20]–[22]. Lee *et al.* used DBD and combined plasma catalysis (CPC) methods to treat SF_6 and studied the effects of different added gases such as Ar, O_2, C_2H_4 and H_2O on degradation. They mainly studied the degradation process of a very low concentration of SF_6(300 ppm). Zhuang *et al.* used a DBD discharge to degrade 820 ppm of SF_6 at 623 ml/m, which the SF_6 degradation rate is close to 100%. Zhang et al. used DBD discharge to degrade SF_6, CF_4 and SF_5CF_3 gases, and analyzed the composition of degradation products by infrared spectroscopy. None of the above studies detected and analyzed active particles in DBD processes by means of optical emission spectrum.

Emission spectrum analysis can effectively obtain parameters such as active particle contents in the plasma region,

2169-3536 © 2018 IEEE. Translations and content mining are permitted for academic research only.
Personal use is also permitted, but republication/redistribution requires IEEE permission.
See http://www.ieee.org/publications_standards/publications/rights/index.html for more information.

and does not interfere with the gas discharge process. It is a common research method for gas discharge phenomena. In 1989, Radovanov *et al.* [23] studied the emission spectrum of $SF_6/N_2/Ar$ under RF discharge. In 1990, *Sadeghi* et.al. studied the production of SF_2 in pure SF_6 over the discharge process by emission spectroscopy [24]. Thereafter, the formation processes of SF_x and F atoms in SF_6 decompositon were studied [25]–[30]. However, the emission spectrum of the SF_6 decomposition process with additional gases (H_2O and O_2) has not been studied.

In this paper, we obtained the emission spectra of SF_6/Ar mixed gas with the participation of O_2 and H_2O, and analyzed the composition of active particles. The decomposition products were detected by fourier transform infrared spectroscopy (FTIR) and gas chromatography-mass spectrometer (GC-MS). Finally, the degradation effect of SF_6 under the participation of H_2O and O_2 was discussed. Relevant research results provide reference for further efficient and harmless treatment of high concentration SF_6.

II. METHOD

A. TEST PLATFORM

The schematic diagram of the DBD plasma system is shown in Figure 1. The plasma is generated by the plasma power supply (CTP-2000K, Nanjing Suman Electronics), with power frequency of 5–20 kHz, operating voltage of 0–30 kV, output power of 0–300 W. The reactor is a concentric double quartz tube. The outer diameter of the inner tube is 8 mm, the thickness of the inner tube is 2 mm. The inner diameter of the outer tube is 20 mm, the thickness of the outer tube is 2.5 mm. The gap distance is 6 mm, the length of the tube is 300 mm and the discharge length is 200 mm. The volume of the discharge area is 86 cm^3. The electrode material is copper.

The reaction gas was mixed by a gas distributor (GC500, Tunkon Electrial Technology Co. Ltd.) with a maximum ratio of 300: 1 and a precision of ±1%FS. The standard gas (Newradargas Co., Ltd, Wuhan) were 10% SF_6, 10% O_2 and 99.999% pure Ar. Ar was used as a carrier gas during this experiment as it has been proven to have a good discharge effect in our previous studies [31]. H_2O was added to the reactor through a gas-washing bottle and the H_2O concentration was measured by a mirror dewpoint meter (GE600, Henan Relations Co., Ltd.). After testing, the temperature of the gas washing-bottle was maintained at about 298 K. Under the flow rate of 50∼100 ml/min, the concentration of H_2O was basically maintained at 0.5%. The treated gas is introduced into the gas-washing bottle with saturated NaOH solution for further treatments.

The concentration of SF_6 was detected by gas chromatograph (GC) (GC-450, Shanghai Huishi Instrument). The concentration of SF_6 was determined by internal peak integration method using a TCD detector. SF_6 peak time is 2.4–2.6 min and the carrier gas is 99.999% high purity Helium. Several decomposition products (SO_2F_2, SOF_2, SO_2 and SOF_4) were quantitatively detected by GC-MS (Shimadzu Ultra 2010plus with CP-Sil 5 CB column, SHIMADZU Co., Ltd.), using the internal peak integration method, 99.999% Helium as the carrier gas. The remaining product was detected by an FTIR (IRTracer-100, SHIMADZU Co., Ltd.) with a detection band of 400-4000 cm^{-1}, with a resolution of 1 nm, and 10 scanning times.

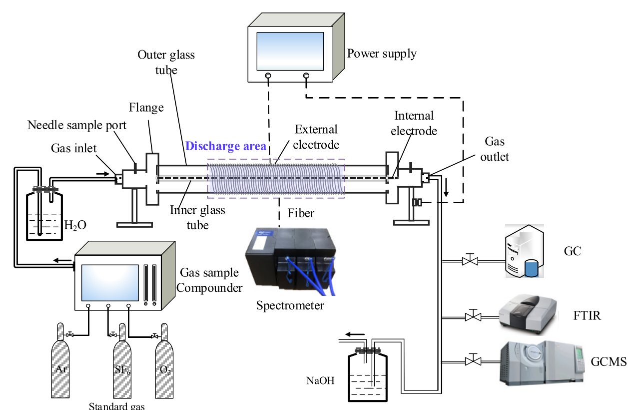

FIGURE 1. Schematic diagram of the DBD plasma system (Input voltage:8-12 kV; Discharge current: 0-0.15 mA; Output power: 0-100 W; Actual discharge length: 20 cm; SF_6 initial concentration: 2%).

The emission spectrum is detected by a three-channel spectrometer (MX2500+, Ocean optics Co., Ltd.), which uses a grating as a beam splitting element and a CCD array as a detector. The wavelength measurement range is 300–800 nm, the optical resolution is 0.1 nm, the integration time is 1 ms–65 s, and the trigger delay and trigger jitter are ± 450 ns and ± 10 ns, respectively.

The experimental conditions are summarized as follows: SF_6 concentration is fixed at 2%. The additives are H_2O (0.5%), O_2(0.5%-8%). The ratio of O_2 to SF_6 was O_2/SF_6 = 1/2-4/1(Volume fraction). The reactor pressure was 101.3 kPa and the mixed gas temperature was 298 K. Power discharge frequency was 8.7 kHz, the input voltage was around 7–13.6 kV. The gas flow rate was controlled at 50 ml/min. The flow rate is relatively low and it's limited by the size of the discharge tube. When considering the practical application, tens of discharge tubes can form a matrix, which greatly increases the flow rate and throughput, and meets the requirements of industrial applications. This is one of our current research works.

B. PARAMETER CALCULATION METHOD

The product compositions were based on molar concentrations of the effluent. The destruction and removal efficiencies of SF_6 (DRE) were calculated as follows:

$$DRE(\%) = \frac{C_{in} - C_{out}}{C_{in}} \tag{1}$$

where C_{in} and C_{out} are the SF_6 concentrations before and after the treatment.

Energy yield (EY) is calculated based on the DRE and the input power P_i. EY is defined as the mass (g) of SF_6

degradation per unit of energy (kWh). The formula is:

$$EY(\mathrm{g/kWh}) = \frac{m_{SF_6converted}}{P_i \times t} \quad (2)$$

Where, $m_{SF6converted}$ is the mass of SF_6, the unit is g. P_i is the input power and is directly read through the display on the voltage regulator table, the unit is kW. t is the reaction time and the unit is h.

The selectivity calculation of the main sulfur-containing by-products is as follows:

$$S_K(\%) = \frac{C_K}{C_{in} - C_{out}} \times 100\% \quad (3)$$

Where K represents the name of the product and C_K is the concentration of the product in the degraded gas.

III. RESULTS AND DISCUSSION

A. DRE AND EY

1) DRE

Figure 2 shows the SF_6 DREs changed with input power under different gas additions. When no H_2O or O_2 was added, the DRE was relatively low. When the input power was 34W, DBD discharge began to occur in the reactor, electrons and active particles reacted with SF_6 to make the S-F bonds broken by equation (4). SF_6 was likely to be recombined by equation (5) and reduced the DRE. When the input power was increased, active particles were accumulated in the discharge area, which resulted in the decomposition process of SF_6 being much faster than that of the recombination process. Meanwhile, SF_x also decomposed continuously by electron collisions, resulting in a significant increase in the DRE. When the input power was 90 W, the DRE reached 60%.

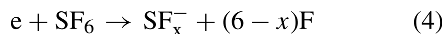

$$e + SF_6 \rightarrow SF_x^- + (6-x)F \quad (4)$$

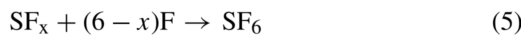

$$SF_x + (6-x)F \rightarrow SF_6 \quad (5)$$

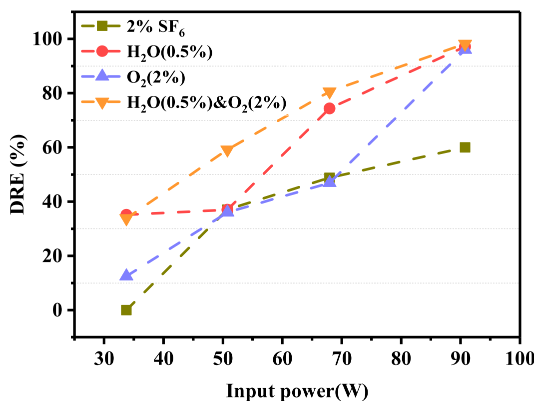

FIGURE 2. Relationship between SF_6 DREs and input power with different gases addition (2% SF_6, 50ml/min).

When O_2 and H_2O were added, the DRE showed a significant increase. The DRE reached 36% under 34W input power with 0.5% H_2O, which may be due to the ionization of H^+ and OH^- in the electric field. The two kind of ions can react with SF_x and restrict the recombination process. Similarly, O_2 can oxidize the SF_x and restricts the recombination process. Therefore, when O_2 or H_2O were added, DRE exceeded 90% under 90W. In Figure 2, when the input power was low, the effect of adding H_2O was better than that of O_2. When the input power was 68W, the DRE under 0.5% H_2O reached 74.37%, while the DRE under 2% O_2 was only 46.91%. The degradation effect with O_2 addition is similar to the degradation effect without it. This may be due to that H_2O is easier to ionize and generates active particles [32]. The low-fluorine sulfides and F^- ions are more likely to react with OH^- and H^+. Besides, when the input power is low, O_2 acts as an electronegative gas, and O_2 ionization in the electric field needs to absorb energy, resulting in a decrease in energy for SF_6 breaking bond decomposition, which affects the DRE. However, when H_2O and O_2 were added together, the DRE was highest, indicating that H_2O and O_2 can simultaneously provide effective active particles and restrict the recombination process.

Besides, we obtained the SF_6 DREs under different O_2 concentrations with input power of 90W. The results are shown in Figure 3.

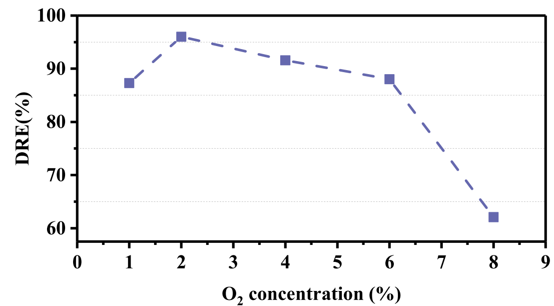

FIGURE 3. Influence of DREs and O_2 concentrations (2% SF_6, 90W input power, 50ml/min).

In Figure 3, the DRE of SF_6 increased firstly and then decreased with the O_2 concentration changing from 1% to 8%. The DRE reached the maximum under 2% O_2 while $c(SF_6)/c(O_2) = 1/1$. The change of O_2 concentration may affect the density of active particles in the discharge area. Too high or too low O_2 concentrations may cause the decrease of active particles, affecting the DRE of SF_6.

Similarly, we maintain the input power of 90W unchanged, adding 0.5% H_2O and changing the concentration of O_2. The DRE change results are shown in Figure 4. In Figure 4, when the O_2 concentration does not exceed 2%, SF_6 has a high DRE, more than 95%. When the O_2 concentration exceeds 4%, the DRE droped rapidly, only 83.81%, indicating that too high concentration of O_2 also had inhibition effect when H_2O was added. Therefore, under this experimental conditions, it is best to keep the ratio of O_2 to SF_6 at 1/1.

The 2% SF_6 DREs under different applied gases were summarized, as shown in Table 1. The flow rate was 50 ml/min and the input power was 90 W. More details about C_{in} and C_{out} are summarized in supplementary data.

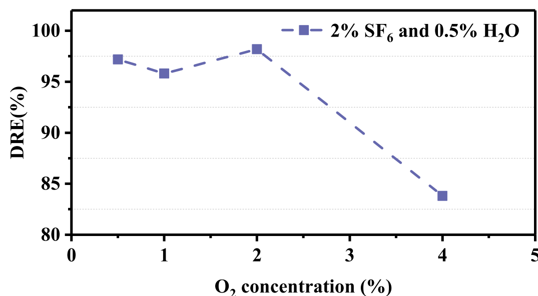

FIGURE 4. Influence of DREs and O_2 concentrations with H_2O addition (2% SF_6, 0.5% H_2O, 90W input power, 50ml/min).

TABLE 1. SF_6 DREs under different additive gas conditions.

Mixtures	DREs	Mixtures	DREs
Without additive	60.0	-	-
H_2O (0.5%)	97.14	O_2(1%)	87.31
H_2O(0.5%)/O_2(0.5%)	97.19	O_2(2%)	96.01
H_2O(0.5%)/O_2(1%)	95.81	O_2(4%)	91.57
H_2O(0.5%)/O_2(2%)	98.19	O_2(6%)	88.02
H_2O(0.5%)/O_2(4%)	83.81	O_2(8%)	62.09

2) EY

According to Equation 2, the EYs of SF_6 degradation were calculated and compared with the related studies [20], [21]. The results are shown in Figure 5.

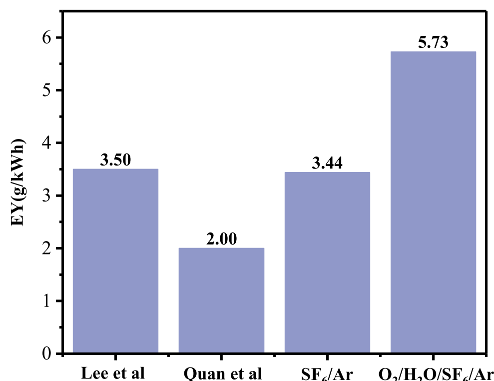

FIGURE 5. EYs for different gases mixture from this study and Lee *et al.* [20] and Quan *et al.* [21].

Compared with [20], [21], this experiment obtained a high DRE of 98.2% and the EY reached 5.73 g/kWh. This may indicate that the coordination between the power supply and the DBD reactor can generate a strong discharge space in the reactor. Meanwhile, with the participation of H_2O and O_2, the active particles were effectively increased and restricted the SF_6 recombination.

B. EMISSION SPECTRA AND BY-PRODUCT ANALYSIS

1) H_2O

Figure 6 is the emission spectrum of the $SF_6/H_2O/Ar$ system. There are many characteristic lines in this figure. The intensity of the line between 700∼800 nm is much larger than other parts. Compared with the NIST database [33], the $SF_6/H_2O/Ar$ plasma emission was initially diagnosed. Several strong main lines in the spectrum are : Ar (696.64 nm), F (739.87 nm), Ar (750.38 nm), Ar (763.51 nm), Ar (794.82 nm), and Ar (800.62 nm). The Ar lines are all I-type, which were generated when the excited state Ar atom transited to a lower energy level.The proportion of Ar in the reaction gas was as high as 97.5%, so the intensity of the lines was relatively large. The production process of these excited state particles Ar∗ is as follows:

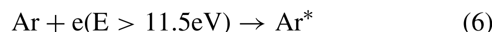

$$Ar + e(E > 11.5eV) \rightarrow Ar^* \quad (6)$$

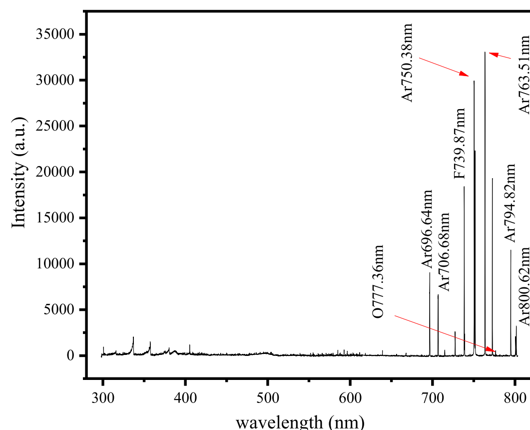

FIGURE 6. The optical emission spectrum of SF_6/ H_2O/Ar plasma (2% SF_6, 0.5% O_2, 97.5% Ar, 10kV, 50ml/min).

The electron energy distribution in the $SF_6/H_2O/Ar$ plasma system were calculated by Zhang *et al.* [31]. The number of electrons in this system with energy greater than 11.5 eV were relatively large, so a large amount of Ar∗ could be produced. In addition to the Ar lines, F I-type line at 739.87 nm was relatively large, which was generated by the dissociation of SF_6 molecules, and the production processes may be following the equations (7)-(9):

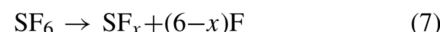

$$SF_6 \rightarrow SF_x + (6-x)F \quad (7)$$

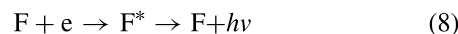

$$F + e \rightarrow F^* \rightarrow F + hv \quad (8)$$

Or

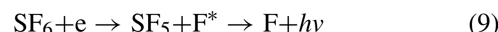

$$SF_6 + e \rightarrow SF_5 + F^* \rightarrow F + hv \quad (9)$$

At the same time, a weak O line was also found at 777.36 nm. In order to analyze the emission spectra of other particles during the discharge, the spectra in the range of 300-450 nm and 450-680 nm were filtered and amplified, as shown in Figures 7(a) and (b), and detailed active particles were analysed.

In the range of 300∼450 nm, the main active particles were OH (308 nm), N_2 (308 nm, 357.61 nm and 380.46 nm), O (362.77 nm), F (385.14 nm), Ar (402.47 nm) and H (434.11 nm). In the range of 450-680 nm, the main active

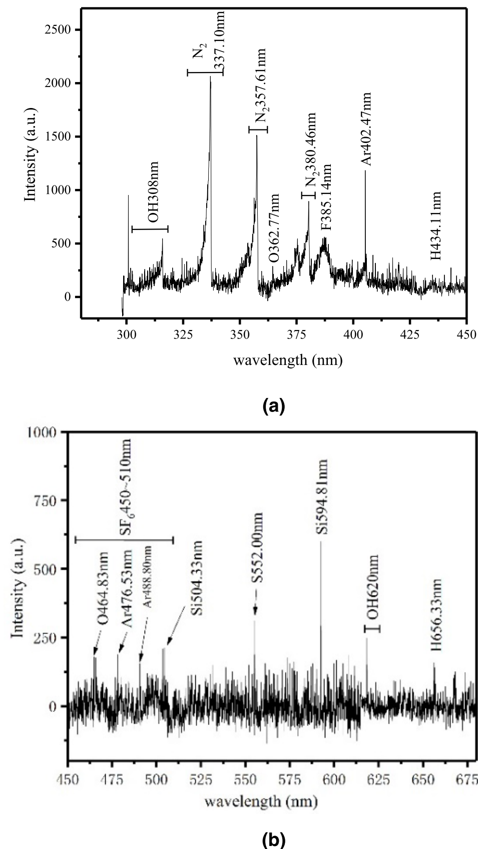

FIGURE 7. The partial emission spectra of $SF_6/H_2O/Ar$ plasma. (a) 300∼450 nm. (b) 450∼680 nm

particles were O (464.83 nm), Ar (476.53 nm and 488.80 nm), S (550.91 nm), OH (620 nm), Si (504.33nm and 594.81 nm) and H (656.33 nm). Moreover, the characteristic peaks of SF_6 molecules were detected at 450∼510 nm, which is consistent with the results of [29]. The source of OH and H radicals is water vapor in the reaction gas, wherein OH is a strong oxidizing group and played an important role in promoting chemical reactions. Since the Si line was detected, it indicates that the active F radicals generated by the dissociation of SF_6 reacted with SiO_2 in the quartz wall. However, the etching process is very slow, and can be neglected when the amount of SF_6 is not large. One reason for using quartz glass as the tube material is to better observe the discharge phenomenon. On the other hand, we has begun to use ceramic tubes as the discharge medium. The ceramic tubes have a similar dielectric barrier effect and are resistant to high temperatures and hardly react with the decomposition products of SF_6, which is suitable for industrial applications. In the semiconductor manufacturing industry, the above reaction is also called the etching reaction. Therefore, O radicals may have two sources, etching of SiO_2 and further decomposition of OH groups. N_2 was absent from the reaction gas, but the band of N_2 was detected in the emission spectrum, and this may because of traces of N_2 leaking into the reactor. Due to the limitations of the emission spectroscopy technique, only the above active particles were detected, but this does not mean that only these active particles are present in the $SF_6/H_2O/Ar$ plasma.

In this experiment, the by-products was qualitatively analyzed using FTIR, and Figure 8 is the FTIR spectrum of the degradation products under 0.5% H_2O. According to Kurte *et al.* [34], [35], the degradation products corresponding to each characteristic peak were determined. In Figure 8, the main products include SOF_2, SOF_4, SO_2F_2, SO_2, SiH_4, SiF_4, SF_4 and S_2F_{10}, similar to the results of Lee *et al.* [20]. Among them, SF_4 and S_2F_{10} are the primary products of degradation, which were directly decomposed by SF_6, and didn't react with H_2O and its free radicals. The presence of SiH_4 and SiF_4 demonstrates that SiO_2 in quartz glass participated in the reaction.

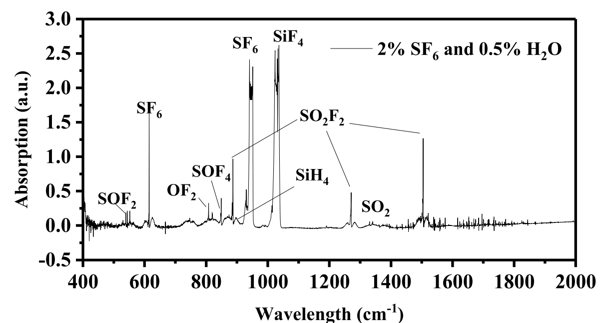

FIGURE 8. FTIR spectrum of by-products under 0.5% H_2O (90W input power, 50 ml/min).

In order to analyse the formation characteristics of by-products, the four products of SOF_4, SO_2F_2, SOF_2, and SO_2 were quantitatively detected by GC-MS, and their selectivity was calculated by equation (3), as shown in Figure 9. SOF_4 is the main product, with the highest selectivity, above 50%. Followed by SO_2, the selectivity is also higher, above 25%, while the production of SO_2F_2 and SOF_2 is smaller. The specific concentration values for the four gases are summarized in the supplementary data.

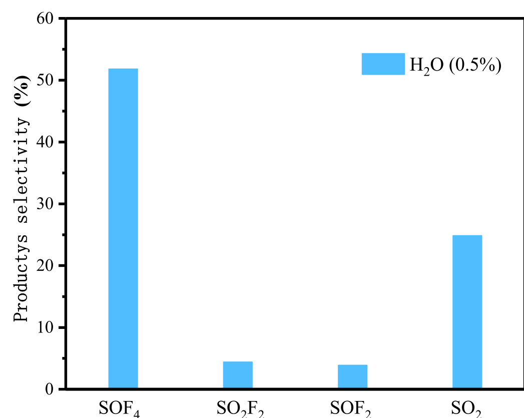

FIGURE 9. Comparison of the selectivity of the main sulphur containing products with H_2O.

2) O_2

In the experiment, the emission spectrum of the $SF_6/O_2/Ar$ system was measured in the range of 300-800 nm. Figure 10 shows the measured emission spectrum, which is very similar to the spectrum of $SF_6/H_2O/Ar$ plasma. The intensity of the line in the range of 690~800 nm is relative large, mainly are Ar, F and O lines.

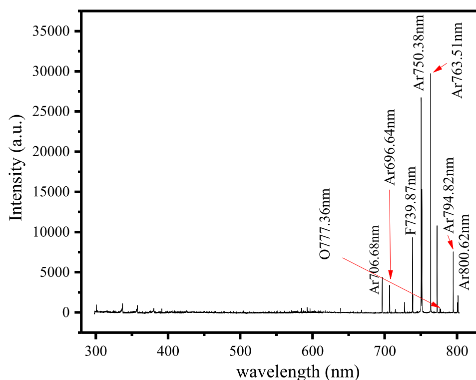

FIGURE 10. The optical emission spectrum of SF_6/ O_2/Ar plasma (2% SF_6, 2% O_2, 96% Ar, 10kV, 50ml/min).

Similarly, the emission spectrum of Figure 10 was filtered and amplified in the range of 300-450 nm and 450-680 nm to obtain detailed information, as shown in Figure 11 (a) and (b). In the 300~450 nm spectrum, the main active particles detected were O (313.57 nm, 362.77 nm, 391.12 nm and 441.12 nm), N_2 (308 nm, 357.61 nm and 380.46 nm), F (385.14 nm) and Ar (427.85 nm). In the range of 450~680 nm, the main active particles detected were O (464.83 nm), Ar (476.53 nm and 488.80 nm), S (550.91 nm) and Si (504.33nm and 594.81 nm). Compared with the $SF_6/H_2O/Ar$ plasma spectrum, since there was no water vapor in the reaction gas, no OH line was detected, but the O lines increased. It can be seen that O radicals are the main strong chemically active groups in the $SF_6/O_2/Ar$ discharge system. Since the Si line was detected, there were also two sources of O radicals. Some water vapor may leak into the reactor and caused the etching reaction of SiO_2. However, there is no SF_6 characteristic peaks at 450~510 nm, which may because SF_6 was degraded thoroughly before the measurement.

Figure 12 is the FTIR spectrum of by-products in $SF_6/O_2/Ar$ system. It can be seen that the main degradation products are SOF_2, SOF_4, SO_2F_2, SO_2, SiF_4, SF_4 and S_2F_{10}. These products were also present under $SF_6/H_2O/Ar$ conditions, but since there were no H-containing particles in the plasma system, no SiH_4 was detected. This also indicates that changes in the applied gas will affect the type of degradation products. The specific concentration values for the four gases are summarized in the supplementary data.

The four products of SOF_4, SO_2F_2, SOF_2, and SO_2 were also quantitatively and their selectivity was calculated, as shown in Figure 13. SOF_4 is still the most important product, with the highest selectivity, above 40%, lower than that in $SF_6/H_2O/Ar$ system. Compared to H_2O conditions,

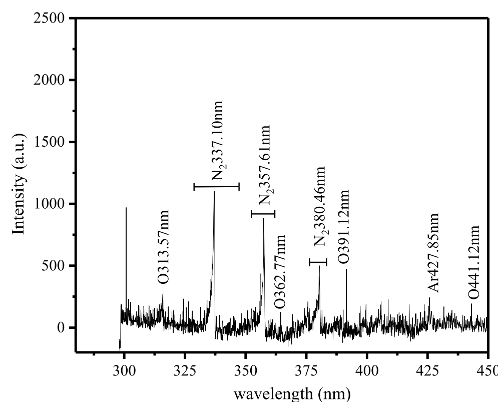

(a)

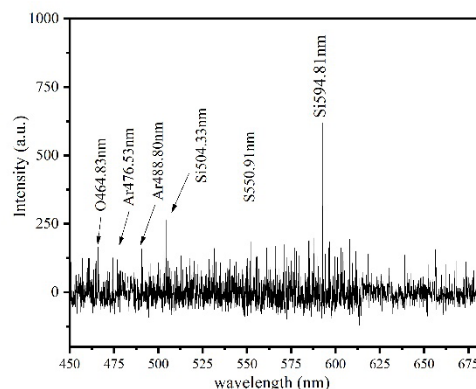

(b)

FIGURE 11. The patrial emission spectrum of SF_6/O_2/Ar plasma. (a) 300~450 nm. (b) 450~680 nm.

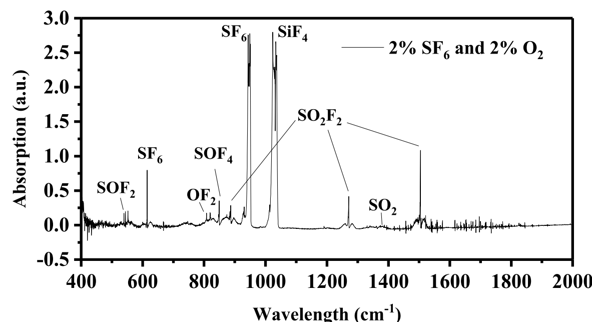

FIGURE 12. FTIR spectrum of by-products under 2% O_2 (90W input power, 50ml/min).

the selectivity of SO_2F_2 was increased by more than 25%, while the selectivity of SO_2 was reduced. Although the selectivity of SOF_2 has increased, it is still low. Therefore, the addition gas not only affects the type of products, but also determines the selectivity of each degradation product.

According to the emission spectra, when H_2O and O_2 participate in the reaction, O, H and OH radicals were generated to react with SF_6 and SF_x to produce products such as SOF_4, SO_2F_2, SOF_2 and SO_2, which hinder the SF_6 recombination process. In Figure 6, the line intensity of H_2O/SF_6/ar

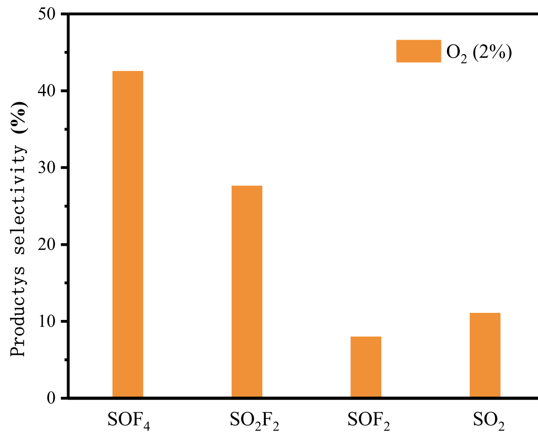

FIGURE 13. Comparison of the selectivity of the main sulphur containing products with O_2.

is stronger than that of $SF_6/O_2/Ar$ in Figure10. This may be because the electronegativity of O_2 is stronger than that of H_2O, and more electrons were adsorbed by O_2 which decreased the spectral intensity.

In our previous work, we've analyzed the possible decomposition paths of SF_6 under the participation of H_2O and O_2 [32]. The reactions involved in the decomposition of SF_6 molecules with additional gases were summarized in Table.2 [32], [35]. Without additional gases, SF_6 caused reactions (10)-(16) in the discharge region and break bonds. Since these reactions are endothermic, the decomposition of SF_6 is relatively slow and recombination reactions may occur to produce SF_6. Adding O_2 will generate a large amount of O radicals in the discharge area, promoted the reactions (17)-(24) and inhibited the recombination process of SF_6, making SF_6 more inclined to produce SO_2F_2 and SOF_2.With H_2O addition. The emission spectra in this experiment can prove that the addition of H_2O will introduce a large amount of H and OH radicals in the discharge region, promoted the reactions (25)-(30), which make SF_6 molecules more inclined to produce SO_2. Meanwhile, reaction(33) will also cause an etching process on the inner wall of the reactor. Beside, the reaction (30) occurred and reduced the SOF_4 production, which is consistent with the Figure 13. Since SO_2F_2 is slightly soluble in water, and SO_2 is easily reacted with an alkali solution [36], SO_2 is more easily treated, so the product with H_2O addition is relatively better than the gas products with O_2 addition.

In this study, 2% SF_6 at a flow rate of 50 ml/min was degraded thoroughly with the participation of H_2O and O_2. The DRE could reach 98.2%. However, the flow rate is relatively low and there are some primary by-products such as SF_4 and S_2F_{10}, indicating that the degradation of SF_6 is not complete. Therefore, designing DBD reactor matrix or using packed bed materials may improve the SF_6 processing efficiency and this is the focus of our current study.

TABLE 2. Formation reations of the by-products and their reaction heat.

No.	Reaction	Reaction heat (kcal/mol)
(10)	$SF_6 + e^* \rightarrow SF_5 \cdot + F \cdot + e$	86.09
(11)	$SF_5 + e^* \rightarrow SF_4 \cdot + F \cdot + e$	41.46
(12)	$SF_4 + e^* \rightarrow SF_3 \cdot + F \cdot + e$	97.15
(13)	$SF_3 + e^* \rightarrow SF_2 \cdot + F \cdot + e$	53.32
(14)	$SF_2 + e^* \rightarrow SF \cdot + F \cdot + e$	86.18
(15)	$SF + e^* \rightarrow S \cdot + F \cdot + e$	113.79
(16)	$2SF_6 + e^* \rightarrow S_2F_{10} + F_2$	118.28
(17)	$SF_5 + O \rightarrow SOF_4 + F$	-42.53
(18)	$SF_4 + O \rightarrow SOF_4$	-126.63
(19)	$SF_2 + O \rightarrow SOF_2$	-130.89
(20)	$SF + O + F \rightarrow SOF_2$	-217.07
(21)	$SOF_2 + O \rightarrow SO_2F_2$	-39.03
(22)	$SO_2F_2 \rightarrow SO_2 + 2F \cdot$	81.26
(23)	$SOF_4 + O \rightarrow SO_2F_2 + 2F$	88.46
(24)	$S + 2O \rightarrow SO_2$	-274.71
(25)	$SF_5 + OH \rightarrow SOF_4 + HF$	4.51
(26)	$SF_4 + OH + F \rightarrow SOF_4 + HF$	-156.64
(27)	$SF_3 + OH \rightarrow SOF_2 + HF$	-107.59
(28)	$SF_2 + OH + F \rightarrow SOF_2 + HF$	-160.91
(27)	$SF + OH + 2F \rightarrow SOF_2 + HF$	-247.09
(29)	$SOF_2 + H_2O \rightarrow SO_2 + 2HF$	-18.33
(30)	$SOF_4 + H_2O \rightarrow SO_2F_2 + 2HF$	-26.35
(31)	$F + F \rightarrow F_2$	-55.95
(32)	$H + F \rightarrow HF$	-145.95
(33)	$HF + SiO_2 \rightarrow SiF_4 + H \cdot + O \cdot$	313.57

IV. CONCLUSION

In this paper, a DBD-based SF_6 decomposition platform is provided, which can effectively degrade high concentration SF_6. The degradation of SF_6 at 2% concentration with H_2O and O_2 involved was studied experimentally. The effects of the two gases on the DRE and EY were studied. The active species and by-products were also analyzed.

The results show that the participation of H_2O and O_2 can effectively promote the DRE of SF_6. The DRE of SF_6 first increased and then decreased with the increase of O_2 concentration. The best degradation effect can be obtained at $SF_6/O_2 = 1/1$. Under the conditions of 0.5% H_2O and 2% O_2, the DRE of 2% SF_6 was 98.2% at 50 ml/min flow rate and the EY reached 5.73 g/kWh.

By the emission spectrum detection, we found a large number of Ar I-type lines were generated in the plasma region. At the same time, the lines of O, OH, F and S were detected in the reaction zone, which indicated that the addition of H_2O and O_2 could effectively produce more active particles like OH, H and O, and promote the bond breaking process of SF_6. In addition, it was found that there was a Si line in $SF_6/H_2O/Ar$ system, indicating that HF was generated during the reaction with H_2O addition, to etch the inner wall of the reactor. The product analysis shows that the addition of H_2O promotes the production of SO_2, while the addition of O_2 promotes the production of SO_2F_2, but SOF_4 is the major decomposition product in both discharge systems.

This paper provided the experimental support for better understanding the decomposition mechanism of SF_6 and the engineering application of SF_6 exhaust gas treatment by using low-temperature plasma.

REFERENCES

[1] R. Ullah, A. Rashid, A. Rashid, F. Khan, and A. Ali, "Dielectric characteristic of dichlorodifluoromethane (R12) gas and mixture with N_2/air as an alternative to SF_6gas," *High Voltage*, vol. 2, no. 3, pp. 205–210, Sep. 2017.

[2] J. Reilly *et al.*, "Multi-gas assessment of the Kyoto protocol," *Nature*, vol. 401, no. 6753, pp. 549–555, 1999.

[3] M. Rabie and C. M. Franck, "Assessment of eco-friendly gases for electrical insulation to replace the most potent industrial greenhouse gas SF_6," *Environ. Sci. Technol.*, vol. 52, no. 2, pp. 369–380, 2018.

[4] S. Xiao, Y. Li, X. Zhang, J. Tang, S. Tian, and Z. Deng, "Formation mechanism of CF_3I discharge components and effect of oxygen on decomposition," *J. Phys. D, Appl. Phys.*, vol. 50, no. 15, p. 155601, 2017.

[5] D. Kashiwagi *et al.*, "Metal phosphate catalysts effective for degradation of sulfur hexafluoride," *Ind. Eng. Chem. Res.*, vol. 48, no. 2, pp. 632–640, 2009.

[6] D. Kashiwagi *et al.*, "Catalytic activity of rare earth phosphates for SF_6 decomposition and promotion effects of rare earths added into $AlPO_4$," *J. Colloid Interface Sci.*, vol. 332, no. 1, pp. 136–144, 2009.

[7] J. Zhang, J. Z. Zhou, Q. Liu, G. Qian, and Z. P. Xu, "Efficient removal of sulfur hexafluoride (SF_6) through reacting with recycled electroplating sludge," *Environ. Sci. Technol.*, vol. 47, no. 12, pp. 6493–6499, 2013.

[8] J. Zhang *et al.*, "Decomposition of potent greenhouse gas sulfur hexafluoride (SF_6) by Kirschsteinite-dominant stainless steel slag," *Environ. Sci. Technol.*, vol. 48, no. 1, pp. 599–606, 2014.

[9] L. Huang *et al.*, "Photoreductive degradation of sulfur hexafluoride in the presence of styrene," *J. Environ. Sci-China.*, vol. 20, no. 2, pp. 183–188, 2008.

[10] X. Song, X. Liu, Z. Ye, J. He, R. Zhang, and H. Hou, "Photodegradation of SF_6 on polyisoprene surface: Implication on elimination of toxic byproducts," *J. Hazardous Mater.*, vol. 168, no. 1, pp. 493–500, 2009.

[11] Y. Yamada, H. Tamura, and D. Takeda, "Photochemical reaction of sulfur hexafluoride with water in low-temperature xenon matrices," *J. Chem. Phys.*, vol. 134, no. 10, p. 104302, 2011.

[12] L. Zámostná and T. Braun, "Catalytic degradation of sulfur hexafluoride by rhodium complexes," *Angew. Chem. Ed.*, vol. 54, no. 36, pp. 10652–10656, 2015.

[13] M. Shih, W.-J. Lee, and C.-Y. Chen, "Decomposition of SF_6 and $H2_S$ mixture in radio frequency plasma environment," *Ind. Eng. Chem. Res.*, vol. 42, no. 13, pp. 2906–2912, 2003.

[14] Y. Kabouzi *et al.*, "Abatement of perfluorinated compounds using microwave plasmas at atmospheric pressure," *J. Appl. Phys*, vol. 93, no. 12, pp. 9483–9496, 2003.

[15] C.-H. Tsai and J.-M. Shao, "Formation of fluorine for abating sulfur hexafluoride in an atmospheric-pressure plasma environment," *J. Hazardous Mater.*, vol. 157, no. 1, pp. 201–206, 2008.

[16] J. H. Kim, C. H. Cho, D. H. Shin, Y. C. Hong, and Y. W. Shin, "Abatement of fluorinated compounds using a 2.45 GHz microwave plasma torch with a reverse vortex plasma reactor," *J. Hazardous Mater.*, vol. 294, pp. 41–46, Aug. 2015.

[17] N. Jiang, N. Lu, K. Shang, J. Li, and Y. Wu, "Effects of electrode geometry on the performance of dielectric barrier/packed-bed discharge plasmas in benzene degradation," *J. Hazardous Mater.*, vol. 262, no. 22, pp. 387–393, 2013.

[18] N. Jiang, N. Lu, K. Shang, J. Li, and Y. Wu, "Innovative approach for benzene degradation using hybrid surface/packed-bed discharge plasmas," *Environ. Sci. Technol.*, vol. 47, no. 17, pp. 9898–9903, 2013.

[19] H. Zhang, K. Li, C. Shu, Z. Lou, T. Sun, and J. Jia, "Enhancement of styrene removal using a novel double-tube dielectric barrier discharge (DDBD) reactor," *Chem. Eng. J.*, vol. 256, no. 8, pp. 107–118, 2014.

[20] H. M. Lee, M. B. Chang, and K. Y. Wu, "Abatement of sulfur hexafluoride emissions from the semiconductor manufacturing process by atmospheric-pressure plasmas," *J. Air Waste Manage.*, vol. 54, no. 8, pp. 960–970, 2004.

[21] Q. Zhuang, B. Clements, A. McFarlan, and Y. Fasoyinu, "Decomposition of the most potent greenhouse gas (GHG) sulphur hexafluoride (SF_6) using a dielectric barrier discharge (DBD) plasma," *Can. J. Chem. Eng.*, vol. 92, no. 1, pp. 32–35, 2014.

[22] R. Zhang, W. Jingting, C. Xu, and H. Huiqi, "Decomposition of potent greenhouse gases SF_6, CF_4 and SF_5CF_3 by dielectric barrier discharge," *Plasma. Sci. Technol.*, vol. 18, no. 4, pp. 388–393, 2016.

[23] S. B. Radovanov, B. Tomčik, Z. L. Petrovič, and B. M. Jelenković, "Optical emission spectroscopy of RF discharge in SF_6," *J. Appl. Phys*, vol. 67, no. 1, pp. 97–107, 1990.

[24] N. Sadeghi, H. Debontride, G. Turban, and M. C. Peignon, "Kinetics of formation of sulfur dimers in pure SF_6 and SF_6-O_2 discharges," *Plasma Chem. Plasma Process.*, vol. 10, no. 4, pp. 553–569, 1990.

[25] M. B. Roque, R. B. Siegel, K. E. Martus, V. Tarnovsky, and K. Becker, "Production of fluorine $^{2,4}P \rightarrow {}^2P^0$ resonance radiation by electron impact on SF_6, CF_4, NF_3, and CCl_2F_2," *J. Chem. Phys.*, vol. 94, no. 1, pp. 341–350, 1991.

[26] A. M. Casanovas *et al.*, "Optical detection of corona discharges in SF_6, CF_4, and SO_2 under DC and 50-Hz AC voltages," *J. Appl. Phys*, vol. 70, no. 3, pp. 1220–1226, 1991.

[27] Z. L. Petrović, F. Tochikubo, S. Kakuta, and T. Makabe, "Spatiotemporal optical emission spectroscopy of RF discharges in SF_6," *J. Appl. Phys*, vol. 73, no. 5, pp. 2163–2172, 1993.

[28] R. Foest, J. K. Olthoff, R. J. Van Brunt, E. C. Benck, and J. R. Roberts, "Optical and mass spectrometric investigations of ions and neutral species in SF_6 radio-frequency discharges," *Phys. Rev. E, Stat. Phys. Plasmas Fluids Relat. Interdiscip. Top.*, vol. 54, no. 2, p. 1876, 1996.

[29] A. Lemzadmi, N. Bonifaci, A. Denat, and M. Nemamcha, "Light emission from corona discharge in SF_6 and SF_6/N_2 gas mixtures at high pressure," *Eur. Phys. J. Appl. Phys.*, vol. 33, no. 3, pp. 213–219, 2007.

[30] S. P. Koirala, I. Awaah, S. L. Burkett, and M. H. Gordon, "Correlation of plasma characteristics to etch rate and via sidewall angle in a deep reactive ion etch system using Langmuir probe and optical emission spectroscopy," *J. Vac. Sci. Technol. A.*, vol. 29, no. 1, pp. 011008-1–011008-6, 2011.

[31] X. Zhang, H. Xiao, X. Hu, and Y. Gui, "Effects of background gas on sulfur hexafluoride removal by atmospheric dielectric barrier discharge plasma," *AIP Adv.*, vol. 6, no. 11, p. 115005, 2016.

[32] H. Xiao, X. Zhang, X. Hu, and Q. Zhu, "Experimental and simulation analysis on by-products of treatment of SF_6 using dielectric barrier discharge," *IEEE Trans. Dielectr. Electr. Insul.*, vol. 24, no. 3, pp. 1617–1624, Jun. 2017.

[33] K. R. Ryan and I. C. Plumb, "Gas-phase combination reactions of SF_4 and SF_5 with F in plasmas of SF_6," *Plasma Chem. Plasma Process.*, vol. 8, no. 3, pp. 281–291, 1988.

[34] *NIST Chemistry WebBook*. [Online]. Available: https://webbook.nist.gov/chemistry/30/09/2018

[35] R. Kurte, C. Beyer, H. Heise, and D. Klockow, "Application of infrared spectroscopy to monitoring gas insulated high-voltage equipment: Electrode material-dependent SF_6 decomposition," *Anal. Bioanal. Chem.*, vol. 373, no. 7, pp. 639–646, 2002.

[36] X. Zhang, H. Xiao, J. Tang, Z. Cui, and Y. Zhang, "Recent advances in decomposition of the most potent greenhouse gas SF_6," *Crit. Rev. Environ. Sci. Technol.*, vol. 47, no. 18, pp. 1763–1782, 2017.

XIAOXING ZHANG was born in Qianjiang, Hubei, China, in 1972. He received the bachelor's and master's degrees from the Hubei Institute of Technology, and the Ph.D. degree from Chongqing University. He is currently a Professor with the School of Electric Engineering, Wuhan University. He is involved in the online monitoring and fault diagnosis of high voltage electrical insulation equipment, alternative gases of SF_6, the decomposition mechanism of insulating gas SF_6, and the new nano-sensor.

ZHAOLUN CUI was born in Binzhou, Shandong, China, in 1993. He received the bachelor's degree in electrical engineering from Wuhan University, Wuhan, China, where he is currently pursuing the Ph.D. degree with the School of Electric Engineering. His research interests include the decomposition mechanism of insulating gas SF_6, and gases spectrum detection technology.

YALONG LI was born in Zhumadian, Henan, China, in 1989. He received the bachelor's degree in electrical engineering from Wuhan University, Wuhan, China, where he is currently pursuing the M.A. degree with the School of Electric Engineering. His research interests include SF_6 abatement technology.

HANYAN XIAO was born in Tianmen, Hubei, China, in 1992. She received the Ph.D. degree in electrical engineering from Chongqing University. She is currently a Senior Engineer with the Electric Power Research Institute, China State Grid Jiangsu Electric Power Co., Ltd. She is involved in the study of the treatment of SF_6 exhaust gas using dielectric barrier discharge.

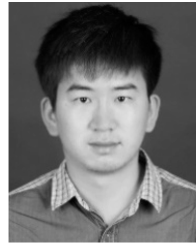

YI LI was born in Shangluo, Shanxi, China, in 1994. He received the bachelor's degree in electrical engineering from Wuhan University, Wuhan, China, where he is currently pursuing the Ph.D. degree with the School of Electric Engineering. His research interests include alternative gas of SF_6 and fault diagnosis of high voltage electrical insulation equipment.

JU TANG was born in Pengxi, Sichuan, China, in 1960. He received the bachelor's degree from Xi'an Jiaotong University, and the master's and Ph.D. degrees from Chongqing University. He is currently a Professor with the School of Electric Engineering, Wuhan University, and a Chief Scientist of the National Basic Research Program of China (973 Program) (2009CB724500). He is involved in high-voltage electric equipment insulation online monitoring and fault diagnosis.